the central metal atom donates its d electrons to H atoms and forms metal-hydrogen bonds. In the nonclassical isomer, the central metal atom retains its d electrons in the d nonbonding orbital. Therefore, the stability of the η^2-H_2 isomer largely depends on the strength of d-electron transfer to H. It can be deduced that for a complex with strong π acceptor ligands and contracted central metal d orbitals, a nonclassical isomer is possibly preferred.

Summary

Examination of different electron correlation techniques for calculating the relative energies of classical and nonclassical hydride isomers suggests that the MP2 method provides a reliable result. The CISD method underestimates the stability of the classical hydride isomer. The effect of basis sets is relatively small when compared with the effect of electron correlation. Therefore, a moderate sized basis set can provide a qualitatively correct result. The conventional substitution of PR_3 ligands by PH_3 in quantum chemical calculations has also been examined for the investigated isomers. In general, PH_3 replacement is a reasonable procedure in this class of transition metal complexes. The electronic structural difference between classical and nonclassical isomers suggest that the nonclassical isomer is preferred for complexes with strong π acceptor ligands and contracted central metal d orbitals.

Acknowledgment. We thank the National Science Foundation (Grant No. CHE 91-13634) and the Robert A. Welch Foundation (Grant No. A-648) for financial support and M. F. Guest for providing the GAMESS package of programs. This research was conducted in part with use of the Cornell National Supercomputer Facility, a resource for the Center for Theory and Simulation in Science and Engineering at Cornell University, which is funded in part by the National Science Foundation, New York State, and the IBM Corp.

Lacunary Polyoxometalate Anions Are π-Acceptor Ligands. Characterization of Some Tungstoruthenate(II,III,IV,V) Heteropolyanions and Their Atom-Transfer Reactivity

Chaoying Rong and Michael T. Pope*

Contribution from the Department of Chemistry, Georgetown University, Washington, D.C. 20057.
Received July 19, 1991

Abstract: Reaction of $[Ru(H_2O)_6]^{2+}$ with $[PW_{11}O_{39}]^{7-}$, followed by oxidation with O_2 yields $[PW_{11}O_{39}Ru^{III}(H_2O)]^{4-}$ (**1**) isolated as the cesium salt. Cyclic voltammetry shows that **1** is reducible/oxidizable to the corresponding aquaruthenium(II) (**2**), oxoruthenium(IV), and oxoruthenium(V) derivatives. The pK_a of **1** is 5.1, determined from a ca. 300 ppm shift of the ^{31}P NMR line between pH 3 and 6. At pH 3.0 and 23 °C the rate of electron transfer between **1** and **2** was determined by ^{31}P NMR line-broadening to be 1.2×10^6 M^{-1} s^{-1}. **2** reacts with pyridine, sulfoxides, dialkyl sulfides, and active alkenes (maleic, fumaric, crotonic acids, 1,4-dihydroxybut-2-ene) to form $[PW_{11}O_{39}Ru^{II}(L)]^{5-}$ species, which are oxidizable to the Ru^{III} stage only. At pH 3.0 and 20 ± 1 °C the half-life for substitution of DMSO for water on **2** is 3.5 h ($k_{obs} = 5.5 \times 10^{-5}$ s^{-1}) and this rate is some 3 orders of magnitude slower than that for water exchange on $[Ru(H_2O)_6]^{2+}$. The electronic spectra of the Ru^{II} derivatives show, in addition to the expected d-d bands, broad intense charge-transfer absorption attributed to $Ru^{II} \rightarrow W^{VI}$. Tungsten-183 NMR spectra of **2** and the dimethyl sulfoxide and maleic acid derivatives show the expected six-line (2:2:2:1:2:2) pattern but with resonances for the W atoms adjacent to Ru deshielded by as much as ca. 360 ppm. This effect is greatest for **2** (L = H_2O) and least for L = maleic acid and is attributed to a partial delocalization of Ru π-electron density onto the polytungstate ligand. The anomalous redox potential for $Ru^{III/II}$ in **2** (in comparison to other $M^{III/II}$ couples in $[PW_{11}O_{39}M(H_2O)]^{5-}$) is a further indicator of electron delocalization. In acidic solution, pH ~ 0, **1** is oxidized to the oxoruthenium(V) derivative in a single two-electron step, and this forms the basis of an electrocatalytic oxidation (40 turnovers) of dimethyl sulfoxide to the sulfone with >90% current efficiency. The tetrabutylammonium salt of **1** in acetonitrile solution catalyzes the epoxidation of *trans*-stilbene by iodosylbenzene. Reduction of **2** to a heteropoly blue is not possible, due to catalytic hydrogen evolution, except in the presence of dimethyl sulfoxide which is catalytically reduced (30 turnovers) to dimethyl sulfide with ca. 50% current efficiency. Preliminary experiments show that the behavior of α_2-$[P_2W_{17}O_{61}Ru^{III}(H_2O)]^{7-}$ parallels that of **1**.

Introduction

The possibility of incorporating transition-metal cations into "octahedral" binding sites on the surfaces of lacunary heteropolyanions such as $[SiW_{11}O_{39}]^{8-}$ and $[P_2W_{17}O_{61}]^{10-}$ (Figure 1) results in the formation of complexes, $[SiW_{11}O_{39}M(L)]^{n-}$ etc., that bear many similarities to metal complexes of macrocyclic ligands, e.g. the metalloporphyrins and related species. This has excited considerable recent interest and activity, for it has been pointed out that the robust nature of the oxometalate "ligands" and their resistance to oxidation lead to valuable potential applications in catalysis, especially since it is possible to work with these species in both polar and nonpolar solvents.[1-5]

(1) (a) Katsoulis, D. E.; Pope, M. T. *J. Am. Chem. Soc.* **1984**, *106*, 2737. (b) Katsoulis, D. E.; Pope, M. T. *J. Chem. Soc., Chem. Commun.* **1986**, 1186. (c) Harmalker, S. P.; Pope, M. T. *J. Inorg. Biochem.* **1986**, *28*, 85. (d) Katsoulis, D. E.; Tausch, V. S.; Pope, M. T. *Inorg. Chem.* **1987**, *26*, 215. (e) Piepgrass, K.; Pope, M. T. *J. Am. Chem. Soc.* **1989**, *111*, 753. (f) Katsoulis, D. E.; Pope, M. T. *J. Chem. Soc., Dalton Trans.* **1989**, 1483.

Table I. Reduction Potentials of $[PW_{11}O_{39}Ru(L)]^{4-/5-}$ and ^{31}P Chemical Shifts of $[PW_{11}O_{39}Ru^{II}(L)]^{5-}$

L	$E(Ru^{III/II})$, V vs SCE	^{31}P, ppm	$\nu_{1/2}$, Hz
Me_2SO	+0.33	−10.8	2.0
$(CH_2)_4SO$	+0.33	−10.8	2.4
Ph_2SO	+0.38	−10.7	2.5
Me_2S	+0.11	−10.8	32
Me-cysteine	+0.17	−10.7	3.2
maleic acid	+0.63	−10.6	2.0
fumaric acid	+0.63	−10.1	1.5
crotonic acid	+0.48	−10.5	2.1
1,4-dihydroxybut-2-ene	+0.41	−10.6	2.5
pyridine	+0.03	−75[a]	1300[a]

[a] Paramagnetic Ru(III) derivative.

When viewed as ligands, heteropolyoxometalates[6] exhibit an unusual combination of properties. The lacunary anions present

0002-7863/92/1514-2932$03.00/0

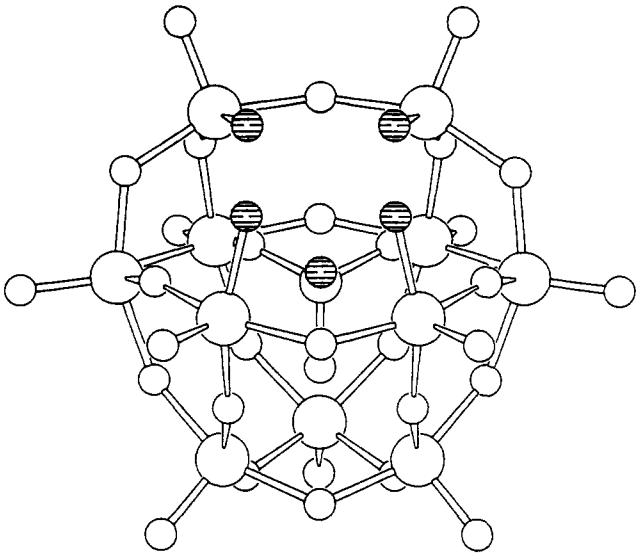

Figure 1. Structure (drawn by SCHAKAL) of a lacunary Keggin anion $[XZ_{11}O_{39}]^{n-}$, Z = Mo, W (large circles). The five oxygen donor atoms lining the lacuna, and which define the octahedral site for M in $[XZ_{11}O_{39}M(L)]^{n-}$, are shown as shaded small circles.

a donor set of "hard" oxide ions (leading to the formation of high-spin complexes of 3d cations), but the adjacent d^0 (Mo^{VI}, W^{VI}) atoms provide "acceptor" orbitals. Furthermore, the extent of backbonding by the substituent atom, and therefore its reactivity, should be modifiable by reduction of the adjacent metal atoms, i.e. by heteropoly blue formation. Such effects are likely to be more noticeable with complexes of second- and third-row transition-metal cations with more extended d orbitals. There have been few reported examples of polyoxometalate–metal complexes of this type that contain a 4d or 5d transition-metal cation,[3,7] and most of these have not been thoroughly characterized. We are in the process of exploring some of these species in more detail, with particular emphasis on those that might be expected to display significant redox and potential catalytic activity. For that reason we have chosen to investigate some ruthenium derivatives.

Experimental Section

Synthesis. Potassium 11-tungstophosphate ($K_7[PW_{11}O_{39}]\cdot xH_2O$) was prepared in a similar way to the 11-tungstosilicate[8] and was identified by IR and ^{31}P NMR spectroscopy. Hexaaquaruthenium(II) *p*-toluenesulfonate, $[Ru(H_2O)_6](C_7H_7SO_3)_2$, was prepared by the literature method,[9] and its purity was checked with cyclic voltammetry (CV) and electronic spectroscopy.

Cesium Undecatungstophospho(aqua)ruthenate(III) (1). To a solution of 0.96 g of $K_7[PW_{11}O_{39}]\cdot xH_2O$ in 50 mL of water at 100 °C under argon was added 0.165 g of $[Ru(H_2O)_6](C_7H_7SO_3)_2$. The solution was stirred at this temperature for 2 h. Ten milliliters of a sulfate buffer solution of pH 3 was added to the resulting hot black solution and dioxygen was then bubbled through for 0.5 h, causing a color change to brown. Upon addition of 1.50 g of CsCl, the cesium salt of the heteropolyanion was precipitated with a yield of 0.90 g. The product was recrystallized from hot water, giving an overall yield of 70%. Anal. Calcd for $Cs_4[PW_{11}O_{39}Ru(H_2O)]\cdot 5H_2O$: Cs, 15.55; P, 0.91; Ru, 2.96; H_2O, 3.17. Found: Cs, 15.58; P, 1.01; Ru, 3.36; H_2O, 2.98. IR(KBr): ν_{as}(P–O), 1088, 1048 cm^{-1} (for PW_{11}, ν_{as}(P–O) = 1084 and 1040 cm^{-1}). NMR: δ/ppm ($\Delta\nu_{1/2}$/Hz); ^{31}P, −87 (300) at pH < 3; ^{183}W, −111.5 (1.4) $^2J_{W\text{-}O\text{-}W}$ = 4.4, 8.2, 19.3 Hz; −146.3 (1.6) $^2J_{W\text{-}O\text{-}W}$ = 4.2, 8.6 Hz; −199.5 (1.8) $^2J_{W\text{-}O\text{-}W}$ = 10.4, 19.5 Hz; −559.5 (21), intensities 2:2:1:2 respectively.

Tetra-*n*-butylammonium Undecatungstophospho(aqua)ruthenate(III). The cesium salt **1** was dissolved in 0.5 M sulfate buffer, pH 3, and a slight excess (5:1 mole ratio) of $(n\text{-}C_4H_9)_4N\cdot HSO_4$ in a small amount of water was added. The resulting brown precipitate was filtered off, washed with water, and recrystallized from acetonitrile. Anal. Calcd for $[(n\text{-}C_4H_9)_4N]_4[PW_{11}O_{39}Ru(H_2O)]\cdot 4H_2O$: C, 20.02; H, 3.75; N, 1.46; H_2O, 2.35. Found: C, 19.76; H, 3.67; N, 1.41; H_2O, 2.44. ^{31}P NMR: −69 ppm (1400 Hz) in CD_3CN.

Undecatungstophospho(aqua)ruthenate(II) (2). A solution of **1** in sulfate buffer, pH 3, was electrolytically reduced on a graphite cloth or platinum gauze electrode at −0.20 V. The resulting solution was characterized by cyclic voltammetry, visible spectroscopy, and NMR. λ_{max}/nm ($\epsilon/M^{-1}\,cm^{-1}$): 385 (2.5×10^3), 530 (2.2×10^3). NMR: ^{31}P, −8.7 ppm (2.6 Hz); ^{183}W (20% D_2O), +291.8, +159.3, −89.1, −102.2, −113.2, −135.8 ppm (2:2:2:1:2:2); all are doublets with $^2J_{P\text{-}O\text{-}W}$ = 1.2–1.8 Hz; line width, 1.0–1.4 Hz.

Tetra-*n*-butylammonium Undecatungstophospho(oxo)ruthenate(IV). A solution of **1** in sulfate buffer, pH 3, was electrolytically oxidized on a graphite cloth electrode at +0.75 V. The resulting aqueous solution was characterized by cyclic voltammetry and ^{31}P NMR, 343 ppm (800 Hz). To this solution a slight excess of $(n\text{-}C_4H_9)_4N\cdot HSO_4$ solution was added. The resulting brown precipitate was filtered off, washed with water, and air-dried. Anal. Calcd for $[n\text{-}(C_4H_9)_4N]_4H[PW_{11}O_{39}RuO]$: C, 20.40; H, 3.85; N, 1.49; P, 0.82. Found: C, 19.47; H, 3.74; N, 1.41; P, 1.00. ^{31}P NMR (CD_3CN): 285 ppm (230 Hz).

Tetra-*n*-butylammonium Undecatungstophospho(dimethyl sulfoxide)ruthenate(II). Method 1. Forty-eight milligrams of **1** was dissolved in 15 mL of 0.5 M sulfate buffer (pH = 3) and electrolytically reduced by one electron at −0.20 V. To this solution was added 0.2 mL of dimethyl sulfoxide (DMSO). The mixture was heated to 70–80 °C under argon for 2 h. λ_{max} 485 nm (ϵ 2.3×10^3). NMR: ^1H 3.34 (s) (cf. 2.73 for free DMSO); ^{31}P −10.8 ppm (2.0 Hz). The brown complex was isolated by adding 0.1 g of tetra-*n*-butylammonium hydrogen sulfate to the solution. The precipitate was washed with water and air-dried. Anal. Calcd for $[n\text{-}(C_4H_9)_4N]_4H[PW_{11}O_{39}Ru(CH_3)_2SO]$: C, 20.71; H, 3.95; N, 1.46; S, 0.84. Found: C, 20.24; H, 3.99; N, 1.41; S, 0.79.

Method 2. Thirty-two milligrams of **1** was dissolved in 10 mL of 0.5 M sulfate buffer, pH 3, and 1 mL of Me_2SO was added. The mixture was kept at 95 °C under argon for 48 h. CV and phosphorus NMR showed the same results as that of method 1.

Tetra-*n*-butylammonium Undecatungstophospho(tetramethylene sulfoxide)ruthenate(II) was prepared analogously by method 1 above. ^{31}P NMR (D_2O): −10.8 ppm (2.4 Hz).

Tetra-*n*-butylammonium Undecatungstophospho(diphenyl sulfoxide)ruthenate(II). Thirty-two milligrams of **1** in 10 mL of 0.5 M sulfate pH 3 solution was reduced to **2**, 0.05 g of diphenyl sulfoxide was then added under Ar, and the solution was heated at 70–80 °C for 6 h. ^{31}P NMR: −10.7 ppm (2.5 Hz). The brown complex was isolated by addition of 0.1 g of tetra-*n*-butylammonium hydrogen sulfate, washed with water, and air-dried.

Undecatungstophospho(dimethyl sulfide)ruthenate(II). Twenty-four milligrams of **1** in 4 mL of 0.5 M sulfate buffer, pH 2.6, was electrolytically reduced by one electron at −0.20 V and 2 mL of dimethyl sulfide was added under argon. The solution was stirred at ca. 40 °C for 6 days. ^{31}P NMR: −10.8 ppm (32 Hz).

Undecatungstophospho(methylcysteine)ruthenate(II). Sixteen milligrams of **1** in 3 mL of 0.5 M sulfate buffer, pH 3, was reduced electrolytically to **2** and transferred to an NMR tube under argon. Eleven milligrams of methylcysteine was added into the tube and the tube was sealed. The phosphorus NMR spectrum initially showed only the signal

(2) (a) Hill, C. L.; Brown, R. B., Jr. *J. Am. Chem. Soc.* **1986**, *108*, 536. (b) Faraj, M.; Hill, C. L. *J. Chem. Soc., Chem. Commun.* **1987**, 1487. (c) Hill, C. L.; Renneke, R. F.; Faraj, M. K.; Brown, R. B., Jr. In The Role of Oxygen in Chemistry and Biochemistry; *Studies in Organic Chemistry*; Ando, W., Moro-oka, Y., Eds.; Elsevier: Amsterdam, 1988; Vol. 33, p 185. (d) Faraj, M.; Lin, C.-H.; Hill, C. L. *New J. Chem.* **1988**, *12*, 745.

(3) (a) Neumann, R.; Abu-Gnim, C. *J. Chem. Soc., Chem. Commun.* **1989**, 1324. (b) Neumann, R.; Abu-Gnim, C. *J. Am. Chem. Soc.* **1990**, *112*, 6025.

(4) (a) Lyon, D. K.; Miller, W. K.; Novet, T.; Domaille, P. D.; Evitt, E.; Johnson, D. C.; Finke, R. G. *J. Am. Chem. Soc.* **1991**, *113*, 7209. (b) Mansuy, D.; Bartoli, J.-F.; Battioni, P.; Lyon, D. K.; Finke, R. G. *J. Am. Chem. Soc.* **1991**, *113*, 7222.

(5) Toth, J. E.; Anson, F. C. *J. Am. Chem. Soc.* **1989**, *111*, 2444.

(6) (a) Souchay, P. *Ions Minéraux Condensés*; Masson: Paris, 1969. (b) Pope, M. T. *Heteropoly and Isopoly Oxometalates*; Springer-Verlag: New York, 1983. (c) Day, V. W.; Klemperer, W. G. *Science (Washington, DC)* **1985**, *228*, 533. (d) Pope, M. T. In *Comprehensive Coordination Chemistry*; Wilkinson, G., Gillard, R. D., McCleverty, J. A., Eds.; Pergamon: Oxford, 1987; Vol. 3; p 1023. (e) Pope, M. T.; Müller, A. *Angew. Chem., Int. Ed. Engl.* **1991**, *30*, 34.

(7) (a) Zonnevijlle, F.; Tourné, C. M.; Tourné, G. F. *Inorg. Chem.* **1982**, *21*, 2751. (b) Ortéga, F.; Pope, M. T. *Inorg. Chem.* **1984**, *23*, 3292. (c) Knoth, W. H.; Domaille, P. J.; Harlow, R. L. *Inorg. Chem.* **1986**, *25*, 1577. (d) Maksimov, G. M.; Maksimovskaya, R. I.; Matveev, K. I. *Russ. J. Inorg. Chem.* **1987**, *32*, 551.

(8) Tézé, A.; Hervé, G. *J. Inorg. Nucl. Chem.* **1977**, *29*, 999.

(9) Bernhard, P.; Biner, M.; Ludi, A. *Polyhedron* **1990**, *9*, 1095.

of **2**; after 3 days this had been replaced by a new line at −10.7 ppm (3.2 Hz). In another 3 days the spectrum remained unchanged. Then the tube was opened and the solution was checked with cyclic voltammetry.

Tetra-*n*-butylammonium Undecatungstophospho(maleic acid)ruthenate(II). Thirty-two milligrams of **1** in 5 mL of 0.5 M sulfate buffer, pH 3, was electrolytically reduced by one electron at −0.20 V. To this solution 0.1 g of maleic acid was added, and the mixture was heated at 70–80 °C for 30 h under argon. λ_{max} 414 nm (ϵ 2.0 × 10^3). ^{31}P, −10.6 ppm (2.0 Hz); ^{183}W (20% D_2O), +64.9, −62.8, −92.5, −109.4, −130.5, −142.4 ppm (2:2:2:1:2:2). The brown complex was precipitated by the addition of 0.1 g of tetra-*n*-butylammonium hydrogen sulfate, washed with water, and air-dried. NMR (CD_3CN): ^{1}H 4.79 (s) (cf. 6.35 free maleic acid).

Tetra-*n*-butylammonium Undecatungstophospho(fumaric acid)ruthenate(II). This complex and the crotonic acid derivative were prepared in a similar manner to the maleic acid derivative. λ_{max} 410 nm (ϵ 2.6 × 10^3). ^{31}P NMR in aqueous solution: −10.1 ppm (1.5 Hz).

Tetra-*n*-butylammonium Undecatungstophospho(crotonic acid)ruthenate(II). λ_{max} 433 nm (ϵ 2.3 × 10^3). ^{31}P NMR in aqueous solution: −10.5 ppm (2.1 Hz).

Undecatungstophospho(1,4-dihydroxybut-2-ene)ruthenate(II). Thirty-two milligrams of **1** in 5 mL of 0.5 M sulfate buffer, pH 3, was electrolytically reduced by one electron to **2** and 0.2 mL of 1,4-dihydroxybut-2-ene was added under Ar. The mixture was heated at 70–80 °C for 30 h and yielded a solution with a single $Ru^{III/II}$ cyclic voltammetric peak, see below, but the ^{31}P NMR spectrum showed traces of other resonances in addition to the major line at −10.6 ppm (2.5 Hz).

Tetra-*n*-butylammonium Undecatungstophospho(pyridine)ruthenate(III). Ninety-six milligrams of **1** in 10 mL of pH 5 acetate buffer (0.5 M) solution was electrolytically reduced by one electron at −0.20 V, 0.2 mL of pyridine was added under argon, and the solution was heated at 70–80 °C for 2 h. λ_{max} 381 (ϵ 6.0 × 10^3), 520 nm (2.5 × 10^3). The Ru^{II} is easily oxidized to Ru^{III} by air, causing a precipitate. Upon warming, the precipitate dissolved and a slight excess of $(n\text{-}C_4H_9)_4N{\cdot}HSO_4$ was then added. The brown tetra-*n*-butylammonium salt was filtered off, washed with water, and air-dried. ^{31}P NMR in CD_3CN: −76 ppm (1300 Hz). Anal. Calcd for $[n\text{-}(C_4H_9)_4N]_4[PW_{11}O_{39}Ru(C_5H_5N)]$: C, 21.65; H, 3.90; N, 1.83. Found: C, 21.19; H, 3.89; N, 1.86.

Physical Measurements. Cyclic voltammetry and controlled-potential coulometry were carried out at room temperature, either on McKee-Pederson modules as described previously[10] or on a BAS 100A electrochemical analyzer. The working electrode was glassy carbon and all potentials were measured relative to the saturated potassium chloride calomel reference electrode. Unless noted otherwise the voltage sweep rate was 2.0 V min^{-1}. The pH was controlled by 0.5 M sulfate and 0.5 M 3,3-dimethylglutarate (plus 0.5 M NaCl) buffers for the pH ranges of 0–3 and 4–7, respectively. For determination of the pK_a of **1** the buffers used were 0.5 M sulfate (0–3), 0.5 M acetate (4–5), and 0.1 M dimethylglutarate (5–7). Infrared spectroscopy was performed on Mattson Galaxy series 2020 FTIR and Nicolet 170SX FTIR instruments. Electronic spectra were obtained on a Cary-14 spectrophotometer. ^{1}H, ^{31}P, and ^{183}W NMR spectra were obtained on a Bruker AM-300WB spectrometer, operating at 7.05 T (300.133 MHz for proton). Resonance frequencies were 121.496 MHz for ^{31}P with 10-mm tubes and 12.505 MHz for ^{183}W with 20-mm tubes. Pulse widths (90°) were 11 μs for ^{31}P and 80 μs for ^{183}W. For paramagnetic species of ^{31}P the sweep widths were 50 000 or 83 333 Hz (acquisition times of 41 and 25 ms, respectively) with an acquisition delay of 100 μs to allow probe ringing to die out. In the case of ^{183}W the acquisition delay was sometimes as long as 500 μs. For diamagnetic species of ^{31}P the sweep widths were 2000 or 4000 Hz (acquisition times of 1.024 and 0.512 s). Chemical shifts are given with respect to external 85% H_3PO_4 and saturated Na_2WO_4. The positive chemical shift is referred to downfield. The tungsten-183 spectra were run on ca. 0.01 M heteropolyanion solutions after cation conversion to lithium.

Results and Discussion

Synthesis and Characterization. $[PW_{11}O_{39}]^{7-}$ reacts with $[Ru(H_2O)_6]^{2+}$ in a straightforward manner because the hexaaquaruthenium(II) is a relatively labile species compared to the Ru^{III} counterpart, but the reaction is still slow in comparison to those of 3d cations. Reaction of $RuCl_3$ with PW_{11} resulted in intransigent mixtures according to ^{31}P NMR spectra and cyclic voltammetry. Following the successful substitution reaction, oxidation of the solution yielded the air-stable and less soluble cesium salt of the tungstoruthenate(III). The combination of

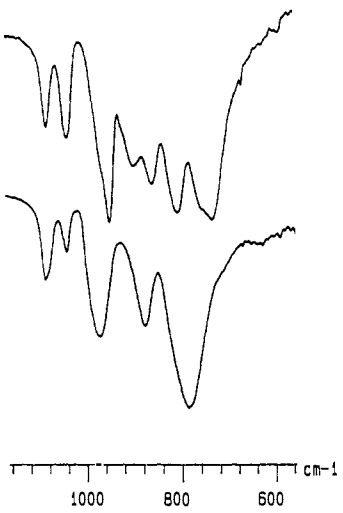

Figure 2. Infrared spectra of $K_7[PW_{11}O_{39}]{\cdot}xH_2O$ (upper) and $Cs_4[PW_{11}O_{39}Ru^{III}(H_2O)]{\cdot}5H_2O$ (lower).

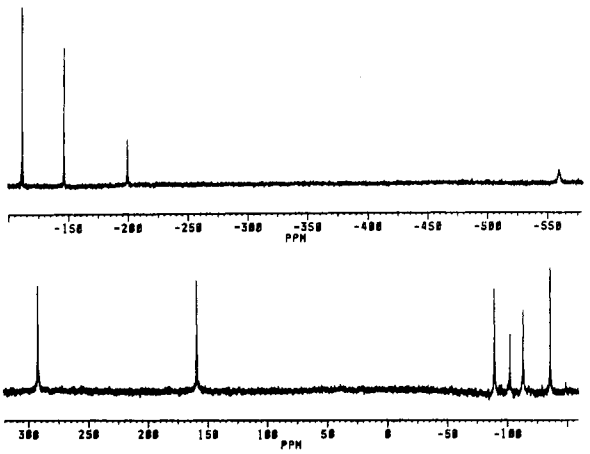

Figure 3. ^{183}W NMR spectra of $[PW_{11}O_{39}Ru^{II}(H_2O)]^{5-}$ (lower) and $[PW_{11}O_{39}Ru^{III}(H_2O)]^{4-}$ (upper).

elemental analysis, IR spectra (Figure 2), and, critically, the six-line ^{183}W NMR spectrum of the Ru^{II} derivative, **2** (Figure 3), generated by stoichiometric controlled potential reduction of **1**, confirms that the Ru^{II} derivative has the anticipated C_s structure of α-$[PW_{11}O_{39}M(H_2O)]^{5-}$. Although six lines would also be expected in the W NMR spectrum of **1**, only four are observed (see Figure 3 and the Experimental Section); the tungsten atoms adjacent to the paramagnetic Ru^{III} center presumably undergo rapid relaxation and are undetectable.

Electrochemistry. Cyclic voltammetry of **1** in acidic solution reveals three reversible redox couples in the range of +1000 to 0 mV (Figure 4a). Controlled potential electrolysis confirmed that each couple corresponded to a single electron transfer and they are therefore assigned to $Ru^{III/II}$, $Ru^{IV/III}$, and $Ru^{V/IV}$. The effects of pH upon the redox potentials are summarized in Figure 5. The $Ru^{III/II}$ and $Ru^{V/IV}$ potentials are pH independent from pH = 0 to 4 and from 1 to 7, respectively. The $Ru^{IV/III}$ potential, however, varies by about 120 mV per pH unit between pH 0 and 4, indicating that two protons are involved in this redox couple. Between pH 5 and 7 the slope becomes 58 mV, corresponding to a single proton change during electron transfer. Another interesting point is that at pH < 1, the two single electron transfers of $Ru^{IV/III}$ and $Ru^{V/IV}$ coalesce to a two-electron transfer (Figure 4b). The electrochemical reactions of the tungstoruthenate are summarized in eqs 1–5. Analogous redox behavior has been documented for polypyridine–oxoruthenium(II–IV) complexes by Meyer et al.[11]

$$[PW_{11}O_{39}Ru^{III}(H_2O)]^{4-} + e^- \rightarrow [PW_{11}O_{39}Ru^{II}(H_2O)]^{5-} \quad \text{pH 0–4} \quad (1)$$

(10) Barrows, J. N.; Pope, M. T. *Adv. Chem. Ser.* **1990**, *No. 226*, 403.

$$[PW_{11}O_{39}Ru^{IV}(O)]^{5-} + e^- + 2H^+ \rightarrow [PW_{11}O_{39}Ru^{III}(H_2O)]^{4-} \quad \text{pH 1–4} \quad (2)$$

$$[PW_{11}O_{39}Ru^{V}(O)]^{4-} + e^- \rightarrow [PW_{11}O_{39}Ru^{IV}(O)]^{5-} \quad \text{pH 0–7} \quad (3)$$

$$[PW_{11}O_{39}Ru^{V}(O)]^{4-} + 2e^- + 2H^+ \rightarrow [PW_{11}O_{39}Ru^{III}(H_2O)]^{4-} \quad \text{pH 0} \quad (4)$$

$$[PW_{11}O_{39}Ru^{IV}(O)]^{5+} + e^- + H^+ \rightarrow [PW_{11}O_{39}Ru^{III}(OH)]^{5-} \quad \text{pH 5–7} \quad (5)$$

^{31}P NMR. The ^{31}P NMR spectra of $[PW_{11}O_{39}Ru^{II}(H_2O)]^{5-}$ (**2**), $[PW_{11}O_{39}Ru^{III}(H_2O)]^{4-}$ (**1**), and $[PW_{11}O_{39}Ru^{IV}(O)]^{5-}$ consist of single lines as expected, with those of the latter two complexes considerably broadened as a result of their paramagnetism. The chemical shift of **1** is extremely pH-dependent, ranging from −80 ppm (pH ≤3) to +234 ppm (pH ≥7) (Figure 6). The titration curve of Figure 6 yields a pK_a of 5.1 for the equilibrium shown in eq 6. The pK_a for hexaaquaruthenium(III), $[Ru(H_2O)_6]^{3+}$, is reported to be 2.4.[12] The difference between the two pK values is attributed to the negative charge of the heteropolyanion.

$$[PW_{11}O_{39}Ru^{III}(H_2O)]^{4-} \rightleftharpoons [PW_{11}O_{39}Ru^{III}(OH)]^{5-} + H^+ \quad (6)$$

It has also been possible to determine the rate of electron exchange between **1** and **2** by ^{31}P NMR line-broadening.[10,13] In preliminary measurements at pH 3.0 (0.5 M sulfate) and 23 °C, spectra of mixtures of 1.30 mM **2** and 0.06–0.26 mM **1** showed two P NMR lines. The electron exchange rate under these conditions, determined from the width of the line from **2**, and using the slow and intermediate exchange limit protocols, was 1.2×10^6 M^{-1} s^{-1}. Further measurements are in progress. The exchange rate for the hexaaqua cations is 20 M^{-1} s^{-1} at 25 °C.[14]

Ligand Substitution. As described in the Experimental Section it was possible to replace the coordinated water molecule of $[PW_{11}O_{39}Ru^{II}(H_2O)]^{5-}$ with several neutral ligands: sulfoxides, diakyl sulfides, pyridine, and active alkenes. To date, we have been unable to demonstrate binding of normal alkenes (cyclohexene, ethylene, 1,3-butadiene, *cis*-butene-2), of carbon monoxide, triphenylphosphine, or dinitrogen. In those cases where ligand substitution occurred, cyclic voltammetry revealed a reversible $Ru^{III/II}$ couple but no further ruthenium oxidations. Potentials and ^{31}P NMR data are summarized in Table I.

It has been shown that it is possible to discriminate between S- and O-bonded dimethyl sulfoxide (DMSO) in $[RuCl_2(dmso)_4]$ on the basis of the change in chemical shift of the protons that occurs on complex formation. For S-bonded DMSO, δ(complex-free) = 1.0 ppm; for O-bonded, δ = 0.12 ppm.[15] In the case of $[PW_{11}O_{39}Ru^{II}(dmso)]^{5-}$, δ = 0.61 ppm and suggests S-bonding.

The replacement of water in **2** by DMSO has been followed by ^{31}P NMR spectroscopy. In the presence of a 100-fold excess of DMSO, substitution follows first-order kinetics for at least 5 half-lives. For 4 mM **2** in 0.5 M sulfate, pH 3.0, 20 ± 1 °C, $k_{obs} = 5.5 \times 10^{-5}$ s^{-1} ($t_{1/2}$ = 3.5 h). To our knowledge this is the first measurement of the rate of ligand substitution on a metal cation embedded in a heteropolyanion. The measured rate is 3 orders of magnitude smaller than that of water exchange on $[Ru(H_2O)_6]^{2+}$, 1.8×10^{-2} s^{-1} at 25 °C.[16] Preliminary investigation of the corresponding substitution on the Ru^{III} heteropoly species, **1**, indicates a rate that is some 2 orders of magnitude slower than for **2**. Further study is in progress.

Proton NMR demonstrates that maleic acid is bound to the heteropolyanion in the expected η^2 mode. The most positive $Ru^{III/II}$ redox potential is observed for the maleic and fumaric acid complexes and is consistent with the strong π-acceptor property of these ligands.[17]

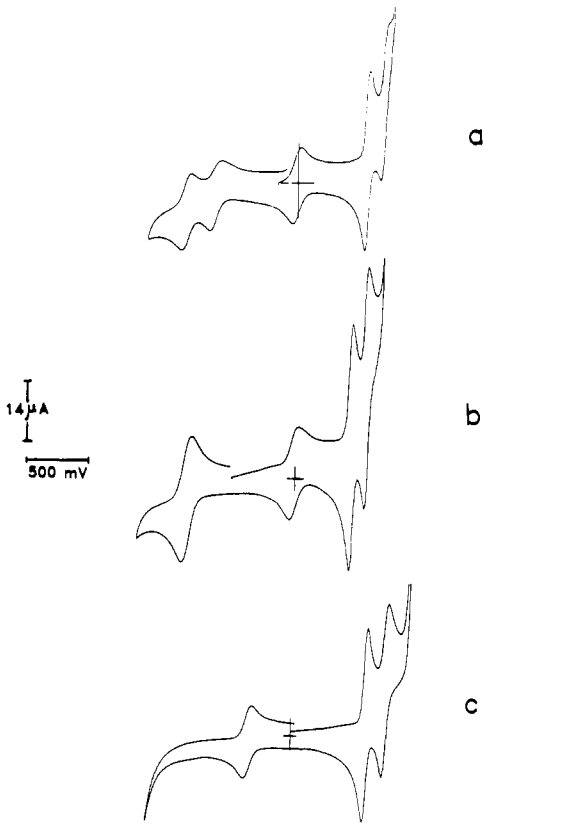

Figure 4. Cyclic voltammograms of (a) $[PW_{11}O_{39}Ru^{III}(H_2O)]^{4-}$, pH 2; (b) $[PW_{11}O_{39}Ru^{III}(H_2O)]^{4-}$, pH 0; and (c) $[PW_{11}O_{39}Ru^{II}(dmso)]^{5-}$, pH 3.

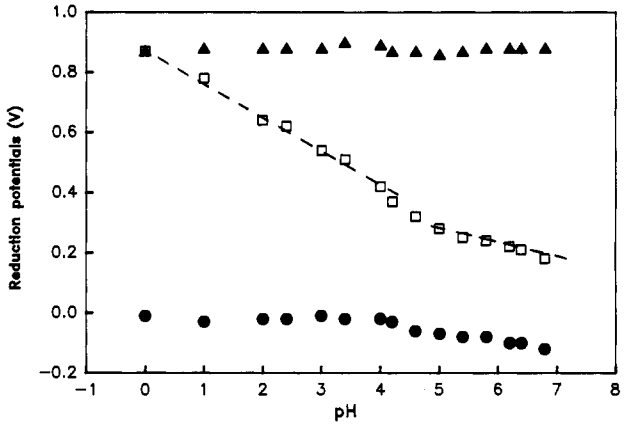

Figure 5. Variation of reduction potentials of $[PW_{11}O_{39}Ru^{III}(H_2O)]^{4-}$ with pH: ●, $Ru^{III/II}$; □, $Ru^{IV/III}$; ▲, $Ru^{V/IV}$; - - -, lines showing ΔE/pH = 120 (60 mV).

Table II. Reduction Potentials of $[M(H_2O)_6]^{3+/2+}$, $[PW_{11}Ru(H_2O)]^{4-/5-}$, and α_2-$[P_2W_{17}Ru(H_2O)]^{7-/8-}$ (V vs SHE)

				ΔE	
M	E- ($M^{III/II}$)	E- ($PW_{11}M^{III/II}$)	E- ($P_2W_{17}M^{III/II}$)	M − $PW_{11}M$	M − $P_2W_{17}M$
Fe	0.77	0.28	0.19	0.49	0.58
Co	1.81	1.39[a]	1.25[b]	0.42	0.56
Mn	1.51	1.12[c]	0.93[c]	0.39	0.58
Ru	0.22	0.21	0.13	0.01	0.09

[a] Reference 20. [b] Reference 21. [c] Reference 22.

(11) Takeuchi, K. J.; Thompson, M. S.; Pipes, D. W.; Meyer, T. J. *Inorg. Chem.* **1984**, *23*, 1845.
(12) Harzion, Z.; Navon, G. *Inorg. Chem.* **1980**, *19*, 2236.
(13) Kozik, M.; Baker, L. C. W. *J. Am. Chem. Soc.* **1990**, *112*, 7604.
(14) Bernhard, P.; Helm, L.; Ludi, A.; Merbach, A. E. *J. Am. Chem. Soc.* **1985**, *107*, 312.
(15) (a) Senoff, C. V.; Maslowsky, E., Jr.; Goel, R. G. *Can. J. Chem.* **1971**, *49*, 3585. (b) Evans, I. P.; Spencer, A.; Wilkinson, G. *J. Chem. Soc., Dalton Trans.* **1973**, 204.
(16) Rapaport, I.; Helm, L.; Merbach, A. E.; Bernhard, P.; Ludi, A. *Inorg. Chem.* **1988**, *27*, 873.
(17) (a) Elliott, M. G.; Shepherd, R. E. *Inorg. Chem.* **1988**, *27*, 3332. (b) Elliott, M. G.; Zhang, S.; Shepherd, R. E. *Inorg. Chem.* **1989**, *28*, 3036.

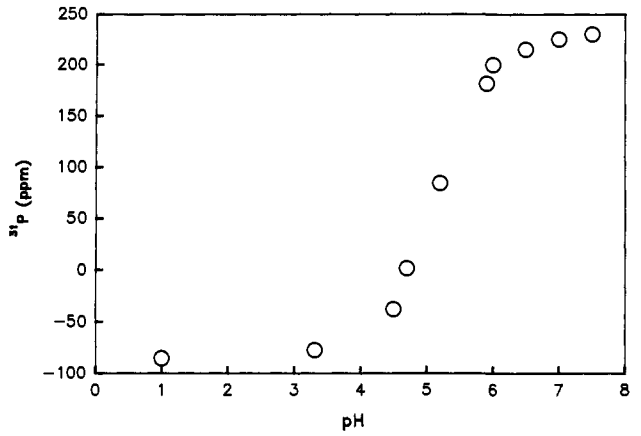

Figure 6. Plot of ^{31}P NMR chemical shifts of $[PW_{11}O_{39}Ru^{III}(H_2O)]^{4-}$ vs pH.

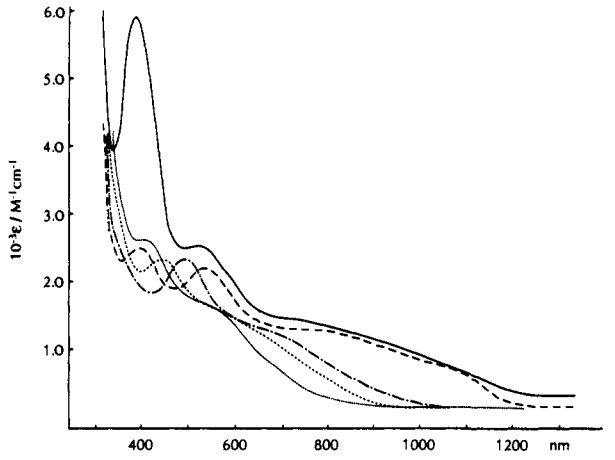

Figure 7. Electronic absorption spectra of Ru^{II} derivatives, $[PW_{11}O_{39}Ru(L)]^{5-}$: pyridine (——); H_2O (– – –); dmso (–·–); crotonic acid (·––); (e) maleic acid (···).

Electronic Spectra. The electronic spectra of several of the Ru^{II} derivatives summarized in Figure 7 show d–d transitions in the expected wavelength range (ca. 400–550 nm) but these are some two orders of magnitude more intense than those of the corresponding simple coordination complexes, $[Ru(H_2O)_6]^{2+}$ etc.[18], as a result of the presence of a broad underlying band that extends into the near-infrared region. This absorption is assigned to a metal-to-"ligand" charge transfer, the ligand in question being the polytungstate. Alternatively this may be described as $Ru^{II} \rightarrow W^{VI}$ charge transfer. The intense band at 381 nm in the spectrum of the pyridine complex is assigned to $Ru^{II} \rightarrow$ pyridine charge transfer. We discuss these spectral features below.

Properties of the Lacunary Polyanion Ligand. Lever[19] has recently analyzed a wide range of $Ru^{III/II}$ redox potentials and proposed a series of additive ligand electrochemical parameters, E_L. For aqueous solution the observed potential, E_{obs}, is given by

$$E_{obs}\ (V) = 1.14[\Sigma E_L] - 0.35$$

Treating $[PW_{11}O_{39}]^{7-}$ as a pentadentate ligand, the data from Table I and ref 19 may be combined to give an average value of 0.06 V for $E_L(PW_{11})$. The significance of this value is unclear in the absence of data for other heteropolyanions.

Of more immediate interest are the potentials listed in Table II. Data are available for four $M^{III/II}$ couples in heteropoly tungstophosphates. We have long since demonstrated that the reduction potentials of the peripheral metal atoms in Keggin anions are strongly influenced by the overall anion charge and that simple Coulombic considerations may be used to rationalize the observed trends.[23] When the overall anion charge is the same, as for $[PW_{11}O_{39}M(H_2O)]^{4-/5-}$, variations of E should parallel those of $[M(H_2O)_6]^{3+/2+}$ if the polytungstate "ligand" is electronically innocent. This is shown to be reasonably true for M = Fe, Co, and Mn, in spite of the variety of electron configurations and spin states involved, by the approximate constancy of the values of ΔE in columns 5 and 6 of Table II. It is also clear from Table II that Ru does not fit the same pattern, and we interpret this result to mean that Ru^{II} is stabilized by about 400 mV in $[PW_{11}O_{39}Ru(H_2O)]^{5-}$ by virtue of its low-spin t_{2g}^6 configuration which permits partial π-delocalization into vacant d orbitals[24] of the adjacent tungsten atoms.

The following other experimental data strongly support the idea of partial electron delocalization:

(1) The existence of a moderately intense Ru → W charge transfer band, the absorption edge of which (for aqua, pyridine, dmso, crotonic acid, and maleic acid derivatives, see Figure 7) correlates with the $Ru^{III/II}$ reduction potentials (Table I).

(2) The Ru → pyridine(π^*) charge transfer band in the spectrum of the heteropolyanion. This band (at 381 nm) appears at higher energy than that for $[Ru(NH_3)_5py]^{2+}$ (407 nm)[25] but at lower energy than that for $[Ru(CN)_5py]^{3-}$ (316 nm)[26] and thereby demonstrates that the polytungstate moiety is intermediate between NH_3 and CN^- as an acceptor ligand.

(3) The tungsten-183 NMR chemical shift data for *diamagnetic* $[PW_{11}O_{39}M^{II}(L)]^{5-}$ which are summarized in Figure 8. The unambiguous assignment for the Zn complex is based on a 2D-INADEQUATE spectrum reported by Jorris et al.[27] The pattern of lines is similar for the Cd and Hg derivatives[28] and suggests analogous assignments. The spectrum of $[PW_{11}O_{39}Ru^{II}(H_2O)]^{5-}$ shows two lines strongly deshielded by ca. 300 ppm, although the remaining four lines are only slightly different from those of the Zn, Cd, and Hg analogues. The two low-field lines are assigned to tungsten atoms 1 and 4 that are adjacent to the ruthenium atom. The positive chemical shifts of these lines are by far the most extreme observed for W^{VI} in diamagnetic polyoxoanions and are consistent with the proposed increase of electron density on W(1) and W(4). (Note that *reduction* of W atoms in heteropolyanions has been shown to lead to downfield shifts, e.g. by 60 ppm in the valence-averaged diamagnetic two-electron heteropoly blue $[SiW_{12}O_{40}]^{6-}$,[29] and by ca. 1600 ppm for W^{IV} in heteropoly "browns"[30]). As shown in Figure 8, replacement of the coordinated water molecule by dimethyl sulfoxide and by maleic acid,[31] results in less extreme chemical shifts for W(1) and W(4) (Figure 8e[32] and f). This can be interpreted in terms of a competition for the Ru π-electrons between the tungstophosphate and the other acceptor ligands.

(4) The rate of electron exchange between **1** and **2** which is some *5 orders of magnitude greater* than for the hexaaqua cations[14] and is comparable to the rates observed for heteropoly-anion/heteropoly blue systems in which the exchanging electron

(18) Mercer, E. E.; Buckley, R. R. *Inorg. Chem.* **1965**, *4*, 1602.
(19) Lever, A. B. P. *Inorg. Chem.* **1990**, *29*, 1271.
(20) Landis, A. L. Ph.D. Dissertation, Georgetown University, 1977. *Diss. Abstr. Int. B* **1978**, *38*, 4225.
(21) Malik, S. A.; Weakley, T. J. R. *J. Chem. Soc. A* **1968**, 2647.
(22) Tourné, C. M.; Tourné, G.; Malik, S. A.; Weakley, T. J. R. *J. Inorg. Nucl. Chem.* **1970**, *32*, 3875.
(23) (a) Pope, M. T.; Varga, G. M., Jr. *Inorg. Chem.* **1966**, *5*, 1249. (b) Altenau, J. J.; Pope, M. T.; Prados, R. A.; So, H. *Inorg. Chem.* **1975**, *14*, 417.
(24) Strictly speaking, not the d orbitals themselves, but the resulting pπ^* orbitals of oxygen atoms bridging Ru and W.
(25) (a) Ford, P. C. *Adv. Chem. Ser.* **1978**, *No. 168*, 73. (b) Ford, P. C.; Rudd, DeF. P.; Gaunder, R.; Taube, H. *J. Am. Chem. Soc.* **1968**, *90*, 1187. (c) Lavallee, D. K.; Baughman, M. D.; Phillips, M. P. *J. Am. Chem. Soc.* **1977**, *99*, 718.
(26) Johnson, C. R.; Shepherd, R. E. *Inorg. Chem.* **1983**, *22*, 2439.
(27) Jorris, T. L.; Kozik, M.; Casan-Pastor, N.; Domaille, P. J.; Finke, R. G.; Miller, W. K.; Baker, L. C. W. *J. Am. Chem. Soc.* **1987**, *109*, 7402.
(28) Fedotov, M. A.; Maksimovskaya, R. I.; Maksimov, G. M.; Matveev, K. I. *Russ. J. Inorg. Chem.* **1987**, *32*, 647.
(29) Kozik, M.; Hammer, C. F.; Baker, L. C. W. *J. Am. Chem. Soc.* **1986**, *108*, 2748.
(30) Piepgrass, K.; Pope, M. T. *J. Am. Chem. Soc.* **1987**, *109*, 1586.
(31) The six-line spectrum for the maleic acid derivative implies fluxional behavior of the alkene ligand. This spectrum and spectra of the other alkene derivatives will be discussed elsewhere.
(32) Liotta, F. Private communication, 1989.

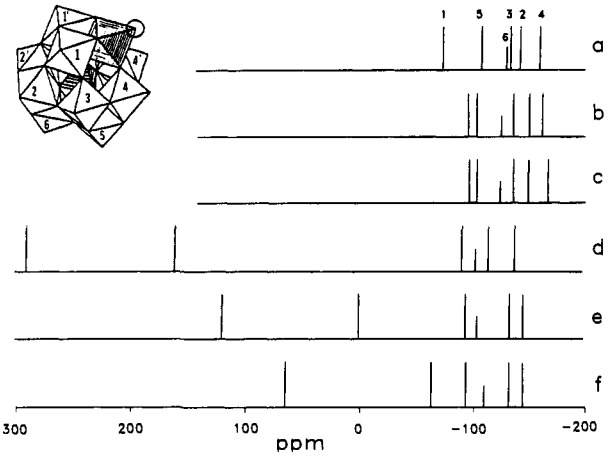

Figure 8. Stick diagrams representing ^{183}W NMR spectra of $[PW_{11}O_{39}M^{II}(L)]^{5-}$, where $M^{II}(L)$ is (a) $Zn(H_2O)$, (b) $Cd(H_2O)$, (c) $Hg(H_2O)$, (d) $Ru(H_2O)$, (e) Ru(dmso), and (f) Ru(maleic acid).

Table III. Electron Exchange Rates for Some Keggin Anions[a]

anion	$k/M^{-1}\ s^{-1}$	μ/M	method	ref
$[PW_{12}O_{40}]^{3-/4-}$	8.2×10^7	0.6	^{31}P	*b*
	1.5×10^6	3.6	^{17}O	*c*
$[PW_{12}O_{40}]^{4-/5-}$	2.5×10^6	1.0	^{31}P	*b*
$[SiW_{12}O_{40}]^{4-/5-}$	6.7×10^5	3.6	^{17}O	*c*
$[PW_{11}O_{39}Ru(H_2O)]^{4-/5-}$	1.2×10^6	1.5	^{31}P	this work

[a] At 25 ± 1 °C. [b] Reference 29. [c] Piepgrass, K. W. Ph.D. Thesis, Georgetown University, 1989; *Diss. Abstr. Int., B* **1990**, *50*, 5059.

is "delocalized" over the 12 tungsten atoms of the Keggin structure; see Table III.

Oxygen Atom Transfer. The coalescence of the $Ru^{IV/III}$ and $Ru^{V/IV}$ oxidation steps of **1** in acid solution (Figure 4b) suggests the possibility of oxygen atom transfer processes involving Ru^V and Ru^{III}. Two kinds of catalytic oxidations have so far been demonstrated: electrolytic oxidation of DMSO to dimethyl sulfone and the oxidation of *trans*-stilbene with iodosylbenzene.

The DMSO oxidation was carried out as follows. One milliliter of a 1% solution of DMSO in water was added to 9 mL of a solution of **1** in 1.0 M H_2SO_4–Na_2SO_4, pH 0. The resulting solution, 14 mM in DMSO and 0.25 mM in **1**, was electrolyzed using a graphite thread anode maintained at +1.10 V for 28 h. The conversion of DMSO to the sulfone was determined by integration of the ^1H NMR peaks at 2.81 and 3.17 ppm in the final solution. The ratio of sulfoxide:sulfone was 0.40, corresponding to the formation of ca. 100 μmol of sulfone and a turnover number of 40 for the catalyst. On the basis of the total quantity of electricity passed, the current efficiency of the oxidation is 92%. When the experiment was repeated using an anodic potential of +0.75 V (i.e. less than the $Ru^{III/V}$ peak potential of +0.95 V) the current efficiency and turnover number fell to 28% and 8, respectively. Electrolysis carried out at +1.10 V in the absence of **1** yielded no sulfone. These results support the following mechanism as a major contributor to the oxidation:

$$[PW_{11}O_{39}Ru^{III}(H_2O)]^{4-} - 2e^- \rightarrow [PW_{11}O_{39}Ru^{V}(O)]^{4-} + 2H^+ \quad (7)$$

$$[PW_{11}O_{39}Ru^{V}(O)]^{4-} + Me_2SO + H_2O \rightarrow [PW_{11}O_{39}Ru^{III}(H_2O)]^{4-} + Me_2SO_2 \quad (8)$$

Alkene oxidations were carried out in acetonitrile solution using *trans*-stilbene as the substrate, iodosylbenzene as oxidant, and $[(n\text{-}C_4H_9)_4N]_4[PW_{11}O_{39}Ru^{III}(H_2O)]$ as the catalyst. The yields of epoxide and benzaldehyde were determined by integration of ^1H NMR peaks at 3.96 and 10.03 ppm, respectively. Other possible products were not identified. Results of these preliminary experiments are shown in Table IV. The table also includes for comparison the results of an experiment using a sample of tetra-*n*-hexylammonium 11-tungstosilicoruthenate(III) that was kindly supplied by Professor Ronny Neumann, who has reported

Table IV. Oxidation of *trans*-Stilbene with Iodosylbenzene in Acetonitrile[a]

catalyst, μmol	substrate, μmol	time/h	yield, μmol	
			epoxide	benzladehyde
5.2 A[b]	220	24[c]	8	62
8.9 A	220	2	44	9
4.2 A	110	2	8	13
3.5 B	110	2	4	1

[a] Conditions: 20 or 40 mg (110 or 220 μmol) of substrate; 50 mg (230 μmol) of PhIO; 16, 20, or 34 mg of catalyst; 5 mL of acetonitrile; 60 °C unless noted otherwise. [b] A, $[(n\text{-}C_4H_9)_4N]_4[PW_{11}O_{39}Ru(H_2O)]\cdot 4H_2O$; B, tetra-*n*-hexylammonium 11-tungstosilicoruthenate(III) (a gift from Professor Neumann). [c] Ca. 25 °C.

elsewhere[3] a much more extensive investigation of the catalytic properties of this tungstosilicate derivative.

Reduction of Dimethyl Sulfoxide. The cyclic voltammograms of the tungstoruthenates show two clearly resolved reversible two-electron reductions of the polytungstate "ligand" (Figure 4). All attempts at controlled potential reduction of $[PW_{11}O_{39}Ru^{II}(H_2O)]^{5-}$ to a two-electron heteropoly blue, using platinum gauze, graphite cloth, or mercury pool cathodes, resulted in catalytic hydrogen reduction. The solution retained the color of the Ru^{II} anion. However, in the presence of DMSO, electrolytic reduction led to a blue solution and to reduction of the sulfoxide. A solution, 14 mM in DMSO and 0.25 mM in $[PW_{11}O_{39}Ru^{III}(H_2O)]^{4-}$ in 0.5 M H_2SO_4–Na_2SO_4, pH 2, was cleanly reduced to the Ru^{II} stage at a graphite cloth electrode (ca. 1 cm^2). The cathode potential was then switched to −0.66 V, beyond the first tungsten reduction peak. Within a few minutes the solution had become dark blue, and after 23 h it was analyzed by proton NMR and cyclic voltammetry. A resonance line at 2.10 ppm (and odor) attested to the formation of dimethyl sulfide. The quantity of DMSO reduced was estimated from ^1H NMR integration to correspond to ca. 30 mol/mol of heteropolyanion. The current efficiency was approximately 50%. No reduction of DMSO occurs in the absence of the heteropolyanion. Cyclic voltammograms of the final electrolyzed solutions showed the presence of both $[PW_{11}O_{39}Ru^{II}(H_2O)]^{5-}$ and $[PW_{11}O_{39}Ru^{II}(dmso)]^{5-}$. These preliminary data are consistent with at least two mechanisms, i.e. delivery of electrons from reduced polytungstate to bound DMSO,[1e,5] or nascent hydrogen reduction of free or bound DMSO. Further investigation of this and related reductions is in progress.

Related Tungstoruthenate Heteropolyanions. Neumann has reported the synthesis of an apparent tungstosilicate analogue of **1** by reaction of $RuCl_3$ with the lacunary anion. Analytical data for potassium and tetra-*n*-hexylammonium salts are good, and these compounds have been shown to be active oxidation catalysts.[3] The cyclic voltammogram of a sample of the potassium salt supplied by Professor Neumann showed multiple poorly resolved features at positive potentials, indicating a possible mixture of closely related species, differing perhaps by the terminal ligand. We have attempted to prepare $[SiW_{11}O_{39}Ru^{III}(H_2O)]^{5-}$ and α_2-$[P_2W_{17}O_{61}Ru^{III}(H_2O)]^{7-}$ by the reaction of $[Ru(H_2O)_6]^{2+}$ with the corresponding lacunary anions, followed by oxidation with dioxygen. The cyclic voltammogram of the apparent silicate derivative showed only traces of $Ru^{IV/III}$ and $Ru^{V/IV}$ waves and this substance has not been studied further. The α_2-$[P_2W_{17}O_{61}Ru^{III}(H_2O)]^{7-}$ derivative was successfully isolated,[33] but it was always contaminated with minor amounts of α-

(33) In one preparation a mixture of 2.34 g of α_2-$K_{10}[P_2W_{17}O_{61}]\cdot nH_2O$ (prepared from α-$[P_2W_{18}O_{62}]^{6-}$ and characterized by IR and ^{31}P NMR spectroscopy) in 8 mL of water and 0.275 g of $[Ru(H_2O)_6](C_7H_7SO_3)_2$ in 2 mL of water was heated under Ar at 100 °C for 7 h. At this stage a cyclic voltammogram and ^{31}P NMR showed that ca. 50% of the phosphorus was present as α-$[P_2W_{18}O_{62}]^{6-}$. The black solution was treated with 2 g of KCl to produce a small quantity of a dark precipitate (containing predominantly the P_2W_{18} anion). Dioxygen was bubbled through the filtrate for 0.5 h, and a second 2-g quantity of KCl was added, followed by filtration. The resulting very dark filtrate was then treated with 0.5 g of CsCl to yield about 1 g of product. the final yield, following recrystallization from hot water, was about 300 mg. ^{31}P NMR of a solution of the product showed that an impurity of 5–10% α-$[P_2W_{18}O_{62}]^{6-}$ remained. This was undetectable in cyclic voltammograms.

$[P_2W_{18}O_{62}]^{6-}$. Experiments were carried out on the mixture. At pH 3 the $Ru^{III/II}$, $Ru^{IV/III}$, and $Ru^{V/IV}$ reduction potentials are −0.11, +0.62, and +0.77 V, respectively. ^{31}P NMR: −17.1 ppm (4.4 Hz), −59.2 ppm (240 Hz). Substitution reactions with DMSO paralled those of $PW_{11}Ru^{II}$ and yielded α_2-$[P_2W_{17}O_{61}Ru^{II}(dmso)]^{8-}$, for which $E(Ru^{III/II})$ = +0.20 V. ^{31}P NMR: −8.7 ppm (7.4 Hz) and −13.5 ppm (7.4 Hz).

Acknowledgment. This work has been supported by the National Science Foundation (CHE 8910921) and ARCO Chemical Co. Dr. Frank Liotta (ARCO) has independently prepared $[PW_{11}O_{39}Ru^{II}(dmso)]^{5-}$, and we thank him for the W NMR spectrum of this complex. We also thank Professor Andreas Ludi for a preprint and helpful advice on the synthesis of $[Ru(H_2O)_6]^{2+}$ and Professor Ronny Neumann for preprints of his catalysis work, for samples of the tungstosilicate derivatives, and for ongoing collaboration. Figure 1 was generated by SCHAKAL 88B/V16 (copyright Egbert Keller, University of Freiburg).

The Persistent Radical Effect: A Prototype Example of Extreme, 10^5 to 1, Product Selectivity in a Free-Radical Reaction Involving Persistent Co^{II}[macrocycle] and Alkyl Free Radicals

Brian E. Daikh and Richard G. Finke*

Contribution from the Department of Chemistry, University of Oregon, Eugene, Oregon 97403.
Received August 26, 1991

Abstract: Thermolysis of the coenzyme B_{12} model complex, **1**, leads to an equilibrium between **1** and the benzyl migration product **2**, but *not* to even a few percent of the usual radical-recombination product bibenzyl, eq 1. Further investigation of this *inter*molecular reaction between freely diffusing radicals has revealed a selectivity of ca. 10^5 to **1** (i.e., 99.999%) for **1** and **2** in comparison to bibenzyl (0.001%). General precedent for this result is found in a seminal paper by Fischer which outlines the criteria for such selectivity, but the present specific example provides a prototypical system for which the actual selectivity factor has been experimentally determined and which has been studied in detail. Numerical integration kinetic modeling of the formation of **2** from **1** over day time periods accurately predicts the formation of trace amounts of bibenzyl, consistent with our experimental results, while modeling over short times (≤100 ms) confirms the major criteria for free-radical selectivity discussed by Fischer. Kinetic modeling over very long times (1000 years) provides the most dramatic illustration to date of Fischer's principle of "internal suppression of fast reactions" (the "persistent radical effect") by showing that only 0.18% of bibenzyl is formed even after a hypothetical 1000 years.

Introduction

Recently we reported the unprecedented benzyl cobalt-to-carbon alkyl migration reaction shown in eq 1.[1-3] A detailed mechanistic study of this reaction[1b] indicated that this apparently *intra*molecular reaction in fact proceeds completely *inter*molecularly via the free-radical intermediates, $PhCH_2^{\bullet}$ and the stable ("persistent"), freely diffusing $^{\bullet}Co^{(II)}$[macrocycle] radical. Excellent evidence for the mechanistic pathway in Scheme I was obtained.[4]

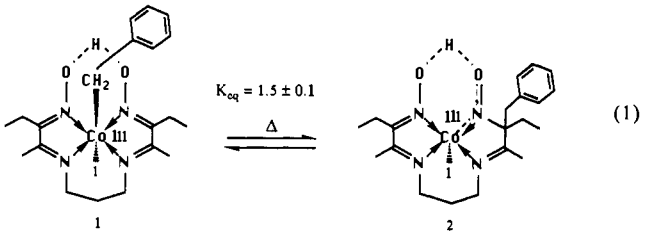

1 2 (1)

One of the few features of Scheme I that was not well understood before[1b] is the expected (but previously unverified and unquantitated) presence of bibenzyl. In fact, our earlier search for bibenzyl by NMR under conditions where 5% or more would have been detected proved negative;[1] this lack of the "expected" bibenzyl product was one of the initial reasons we chose to pursue this research.[4b]

In 1986, a seminal paper by Fischer appeared which included insightful suggestions by Ingold.[5a] This paper discussed, in a general way, how such free-radical reactions could be highly selective if two criteria were fulfilled:[5] (1) of the radical intermediates formed during the course of the reaction in question, one must be more persistent than the others, and (2) the persistent

(1) (a) Daikh, B. E.; Hutchison, J. E.; Gray, N. E.; Smith, B. L.; Weakley, T. J. R.; Finke, R. G. *J. Am. Chem. Soc.* **1990**, *112*, 7830. (b) Daikh, B. E.; Finke, R. G. *J. Am. Chem. Soc.* **1991**, *113*, 4160. (c) Daikh, B. E. University of Oregon Honors College Undergraduate Thesis, Eugene, OR, May 9, 1990.

(2) A study of the low, ca. 25 kcal/mol C-benzyl bond dissociation energy in **2**: Daikh, B. E.; Finke, R. G. *J. Chem. Soc., Chem. Commun.* **1991**, 784.

(3) An X-ray crystallographic investigation of the bonding changes accompanying the rearrangement of **1** to **2**: Daikh, B. E.; Weakley, T. J. R.; Finke, R. G. *Inorg. Chem.* **1992**, *31*, 137.

(4) (a) The mechanistic evidence includes (but is not limited to[1b]) a rate law starting with **1**, and with added free radical trap TEMPO (2,2,6,6-tetramethylpyridinyloxy free radical), that is inversely dependent on $^{\bullet}Co^{(II)}$[macrocycle] and zero-order in added TEMPO[4b] (under conditions where the added TEMPO traps 100% of the benzyl radicals, i.e., where TEMPO appears in 100% of the products), demonstrating rate-determining Co-benzyl homolysis in **1**, and a rate law starting with **2** that is similarly zero-order in TEMPO under conditions where TEMPO appears in all the products, consistent with rate-determining C-benzyl homolysis in **2**.[1b] These and other data[1b] provide strong evidence for the mechanism shown in Scheme I. (b) Finke, R. G.; Smith, B. L.; Mayer, B. J.; Molinero, A. A. *Inorg. Chem.* **1983**, *22*, 3677.

(5) (a) Fischer, H. *J. Am. Chem. Soc.* **1986**, *108*, 3925. (b) Selectivities of ca. 4:1 have been reported: Rüegge, D.; Fischer, H. *Int. J. Chem. Kinet.* **1989**, *21*, 703.

0002-7863/92/1514-2938$03.00/0